Electrochemical and Molecular Docking Studies on Benzo[d]Oxazole Derivatives as Corrosion Inhibitors for Mild Steel in Hydrochloric Acid Medium

Hala.M.Hassan[1], A.Attia [2] , Hussain Almalki[3], Marwa .R. Elsayad[4] and A.M.Eldesoky*[5]

[1]Textile Technology Department, Industrial Education College, Beni-Suef University, Egypt and Chemistry Department, Faculty of Science, Jazan University, KSA.

[2] Department of Chemistry, Faculty of Science, Mansoura University, Mansoura, Egypt and Faculty of Science and Arts in Balgarn, Chemistry Department, Bisha University, KSA.

[3] Al-Qunfudah Center for Scientific Research (QCSR), Chemistry Department, Al-Qunfudah University College, Umm Al-Qura University, KSA.

[4] Ophthalmology Dept., Faculty of Medicine, Mansoura University, Egypt and Al-Qunfudah Center for Scientific Research (QCSR), Chemistry Department, Al-Qunfudah University College, Umm Al-Qura University, KSA.

[5] Engineering Chemistry Department, High Institute of Engineering &Technology (New Damietta), Egypt and Al-Qunfudah Center for Scientific Research (QCSR), Chemistry Department, Al-Qunfudah University College, Umm Al-Qura University, KSA.

*Corresponding author: E-mail: a.m.eldesoky79@hotmail.com

Abstract—The inhibitive effect of newly synthesized benzo[d]oxazole derivatives (1-2) against Mild Steel and its adsorption behavior were investigated in 2 M HCl solution using potentiodynamic polarization, electrochemical impedance spectroscopy (EIS) and electrochemical frequency modulation (EFM) techniques. The results showed that the inhibition efficiency increased with the increase of the inhibitor concentration. The benzo[d]oxazole derivatives are a mixed-type inhibitor. The quantum chemistry was used to gain some insight, about structural and electronic effects in relation to the inhibiting efficiencies. EIS spectra exhibit one capacitive loop and confirm the inhibitive ability. Molecular docking was used to predict the binding between benzo[d]oxazole derivatives (1-2) and the receptor of breast cancer mutant 3hb5-oxidoreductase.

Keywords- Breast cancer, Benzo[d]oxazole, EIS, Molecular docking.

———————————————— ◆ ————————————————

1 INTRODUCTION

Acid solutions are widely used in industry, such as acid pickling of iron and steel, chemical cleaning and processing, ore production and oil well acidification [1–3]. The problems arising from acid corrosion required the development of various corrosion control techniques among which the application of chemical inhibitors has been acknowledged as most economical method for preventing acid corrosion [4–9]. Many organics, such as quaternary ammonium salts, acetylenic alcohol, and heterocyclic compounds are widely used as inhibitors in various industries. The organic molecules adsorb on the metal surface through heteroatom, such as nitrogen, oxygen and sulfur, blocking the active sites and generating a physical barrier to reduce the transport of corrosive species to the metal surface [10–16]. Other researches revealed that the adsorption is influenced not only by the nature and surface charge of the metal, but also by the chemical structure of inhibitors. Among these organic compounds, heterocyclic substances containing nitrogen atoms, such as 4-aminoantipyrine compounds are considered to be excellent corrosion inhibitors in combating acidic corrosiondue to high inhibition efficiency, good thermal stability and lack of irritating odor for many metals and alloys in various aggressive media [17–22]. Therefore, the develop of novel modified inhibitors containing 4-aminoantipyrineheterocyclic ring and the study of the relations between the chemicalstructure of inhibitors and their inhibition performances are of great importance, both from the industrial and theoretical points of view.

This paper aims to investigate the inhibition effect and electrochemical behavior of newly synthesized benzo[d]oxazole derivatives (1-2) for Mild Steel in 2 M HCl solution by the potentiodynamic polarization, electrochemical impedance spectroscopy (EIS) and electrochemical frequency modulation (EFM) techniques. Several quantum-chemistry calculations have been performed in order to relate the inhibition efficiency to the molecular properties of the different types of compounds [23–25]. Molecular docking was used to predict the binding between benzo[d]oxazole derivatives (1-2) and the receptor of breast cancer mutant 3hb5-oxidoreductase.

2. Experimental

2.1 Measurements

In the study simulates the actual docking process in which the ligand–protein pair-wise interaction energies are
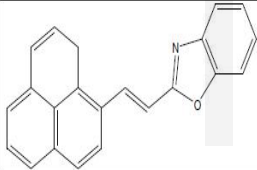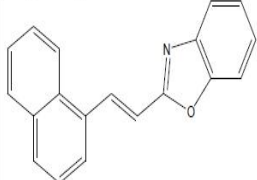
calculated using Docking Server [26]. The MMFF94 Force field was for used energy minimization of ligand molecule using Docking Server. Gasteiger partial charges were added to the compounds (1-2) atoms. Non-polar hydrogen atoms were merged, and rotatable bonds were defined. Docking calculations were carried out on compounds (1-2) protein model. Essential hydrogen atoms, Kollman united atom type charges and solvation parameters were added with the aid of Auto-Dock tools [27]. Auto Dock parameter set- and distance-dependent dielectric functions were used in the calculation of the van der Waals and the electrostatic terms, respectively.

2.2. Material and Medium

Mild Steel was used for the corrosion measurement. Its composition (wt%) is 0.20 C, 0.30 Si, 0.53 Mn, 0.055S, 0.045P, Fe balance. The aggressive solution (2 M HCl) was prepared by dilution of HCl (analytical grade, 37%) with double distilled water. The benzo[d]oxazole derivatives used for this study, whose structures were shown in Table (1) as following [28]:

TABLE 1

CHEMICAL STRUCTURE, NAME, MOLECULAR WEIGHT AND MOLECULAR FORMULA OF INHIBITORS.

Compound No.	Structure	Name	Mol. Wt. / M. Formula
(1)		2-((1E)-2-(1H-phenalen-9-yl)vinyl)benzo[d]oxazole	309 / $C_{22}H_{15}NO$
(2)		2-((E)-2-(Naphthalen-1-yl)vinyl)benzo[d]oxazole	271 / $C_{19}H_{13}NO$

2.3. Methods

2.3.1. Electrochemical Measurements

Electrochemical measurements were conducted in a conventional three electrodes thermostated cell assembly using a Gamrypotentiostat/galvanostat/ZRA (model PCI300/4). A platinum foil and saturated calomel electrode (SCE) were used as counter and reference electrodes, respectively. The Mild Steel electrodes were 1x1 cm and were welded from one side to a copper wire used for electrical connection. The electrodes were abraded, degreased with acetone, rinsed with bidistilled water and dried between filter papers. All experiments were carried out at temperature (30 ± 1 ºC). The potentiodynamic curves were recorded from -500 to 500 mV at a scan rate 1 mV S-1 after the steady state is reached (30 min) and the open circuit potential (OCP) was noted. The % IE and degree of surface coverage were calculated from Eq. (1):

$$\% \ IE \ = \theta \ x \ 100 = [1 - (i°_{corr}/ \ i_{corr} \ )] \ x \ 100 \tag{1}$$

Where $i°_{corr}$ and i_{corr} are the corrosion current densities of uninhibited and inhibited solution, respectively.

Electrochemical impedance spectroscopy (EIS) and electrochemical frequency modulation (EFM) experiments were carried out using the same instrument as before with a Gamry framework system based on ESA400. Gamry applications include software EIS300 for EIS measurements and EFM140 for EFM measurements; computer was used for collecting data. EchemAnalyst 5.5 Software was used for plotting, graphing and fitting data. EIS measurements were carried out in a frequency range of 100 kHz to 10 mHz with amplitude of 5 mV peak-to-peak using ac signals at respective corrosion potential. EFM carried out using two frequencies 2 and 5 Hz. The base frequency was 1 Hz. In this study, we use a perturbation signal with amplitude of 10 mV for both perturbation frequencies of 2 and 5 Hz.

2.3.2 Theoretical Study

Accelrys (Material Studio Version (4.4) software for quantum chemical calculations has been used.

3. Results and Discussion

3.1 Potentiodynamic Polarization Measurements

Polarization measurements were carried out in order to gain knowledge concerning the kinetics of the cathodic and anodic reactions. Figure (1): shows the polarization behavior of Mild Steel electrode in 2 M HCl in the absence and presence of various concentrations of compound (1). Figure (1) shows that both the anodic and cathodic reactions are affected by the addition of investigated benzo[d]oxazole derivatives and the inhibition efficiency increases as the inhibitor concentration increases, but the cathodic reaction is more inhibited, meaning that the addition of benzo[d]oxazole derivatives reduces the anodic dissolution of Mild Steel and also retards the cathodic reactions. Therefore, investigated benzo[d]oxazole derivatives are considered as mixed type inhibitors.

The values of electrochemical parameters such as corrosion current densities (i_{corr}), corrosion potential (Ecorr), the cathodic Tafel slope (βc), anodic Tafel slope (βa) and inhibition efficiency (% IE) were calculated from the curves of Figure (1) and are listed in Table (2). The results in Table (2) revealed that the corrosion current density decreases obviously after the addition of inhibitors in 2 M HCl and % IE increases with increasing the inhibitor concentration. In the presence of inhibitors Ecorr was enhanced with no definite trend, indicating that these compounds act as mixed–type inhibitors in 2 M HCl.
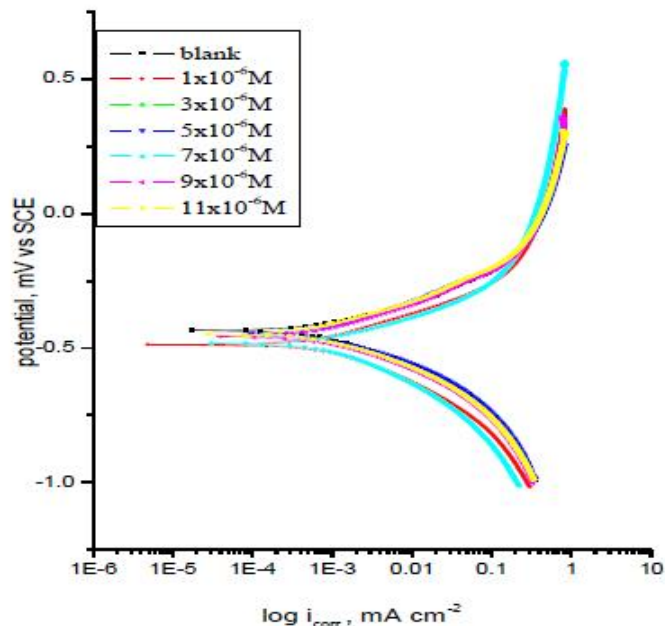
Fig.1: Potentiodynamic polarization curves for the corrosion of Mild Steel in 2 M HCl in the absence and presence of various concentrations of compound (1) at 30 ± 0.1 °C.

TABLE 2

EFFECT OF CONCENTRATIONS OF THE INVESTIGATED BEN-ZO[D]OXAZOLE DERIVATIVES (1-2) ON THE FREE CORROSION POTEN-TIAL (E_{CORR}.), CORROSION CURRENT DENSITY (i_{CORR}.), TAFEL SLOPES (BA & BC), DEGREE OF SURFACE COVERAGE (Θ) AND INHIBITION EFFI-CIENCY (% IE) FOR MILD STEEL IN 2 M HCL AT 30 ± 0.1 °C.

Conc., M		$i_{corr} \times 10^{-4}$, mA cm^{-2}	$-E_{corr}$ mV vs(SCE)	$\beta_a \times 10^{-3}$, mV dec^{-1}	$\beta_c \times 10^{-3}$, mV dec^{-1}	θ	% IE
2 M HCl		6.80	436	109	152	-	-
Compound (1)	1×10^{-6}	3.89	471	188	176	0.4279	42.79
	3×10^{-6}	3.46	453	89	108	0.4911	49.11
	5×10^{-6}	2.99	442	88	125	0.5603	56.03
	7×10^{-6}	1.37	487	52	65	0.7985	79.85
	9×10^{-6}	1.29	488	38	58	0.8103	81.03
	11×10^{-6}	1.01	424	131	243	0.8515	85.15
Compound (2)	1×10^{-6}	5.87	456	19	90	0.1368	13.68
	3×10^{-6}	4.97	456	92	96	0.2691	26.91
	5×10^{-6}	4.63	478	41	32	0.3191	31.91
	7×10^{-6}	4.27	482	89	72	0.3721	37.21
	9×10^{-6}	3.26	443	112	91	0.5206	52.06
	11×10^{-6}	3.14	411	42	32	0.5382	53.82

It is obvious from Table (2) that the slopes of the anodic (βa) and cathodic (βc) Tafel lines remain almost unchanged upon addition of benzo[d]oxazole derivatives, giving rise to a nearly parallel set of anodic lines, and almost parallel cathodic plots results too. Thus the adsorbed inhibitors act by simple blocking of the active sites for both anodic and cathodic processes. In other words, the adsorbed inhibitors decrease the surface area for corrosion without affecting the corrosion mechanism of Mild Steel in 2 M HCl solution, and only causes inactivation of a part of the surface with respect to the corrosive medium [29,30]. The inhibition efficiency of these compounds follows the sequence: compound (1) > compound (2). This sequence may attribute to free electron pair in nitrogen atom, π electrons on aromatic nuclei and the substituent in the molecular structure of the inhibitor.

3.2. Electrochemical Impedance Spectroscopy (EIS)

EIS is well-established and powerful technique in the study of corrosion. Surface properties, electrode kinetics and mechanistic information can be obtained from impedance diagrams [31-35]. Figure (2) shows Nyquist (a) and Bode (b) plots obtained at open-circuit potential both in the absence and presence of increasing concentrations of investigated benzo[d]oxazole derivatives at 30 ± 0.1 °C. The increase in the size of the capacitive loop with the addition of benzo[d]oxazole derivatives shows that a barrier gradually forms on the copper surface. The increase in the capacitive loop size Figure 2(a) enhances, at a fixed inhibitor concentration, following the order: compound (1) > compound (2), confirming the highest inhibitive influence of compound (1).

The Nyquist plots do not yield perfect semicircles as expected from the theory of EIS. The deviation from ideal semicircle was generally attributed to the frequency dispersion [36] as well as to the inhomogenities of the surface. EIS spectra of the benzo[d]oxazole additives were analyzed using the equivalent circuit, Figure (3), which represents a single charge transfer reaction and fits well with our experimental results. The constant phase element, CPE, is introduced in the circuit instead of a pure double layer capacitor to give a more accurate fit [37]. The double layer capacitance, Cdl, is calculated from Eq. (2):

$$Cdl = Yo \, \omega n\text{-}1 / \sin [n \, (\pi/2)] \tag{2}$$

where Yo is the magnitude of the CPE, ω = 2πfmax, fmax is the frequency at which the imaginary component of the impedance is maximal and the factor n is an adjustable parameter that usually lies between 0.50 and 1.0.

After analyzing the shape of the Nyquist plots, it is concluded that the curves approximated by a single capacitive semicircle, showing that the corrosion process was mainly charged-transfer controlled [38-40]. The general shape of the curves is very similar for all samples (in presence or absence of inhibitors at different immersion times) indicating that no change in the corrosion mechanism [41]. From the impedance data (Table 3), we conclude that the value of Rct increases with increasing the concentration of the inhibitors and this indicates an increase in % IE. In fact, the presence of inhibitors enhances

the value of Rct in acidic solution. Values of double layer capacitance are also brought down to the maximum extent in the presence of inhibitor and the decrease in the values of CPE follows the order similar to that obtained for icorr in this study. The decrease in CPE/Cdl results from a decrease in local dielectric constant and/or an increase in the thickness of the double layer, suggesting that benzo[d]oxazole derivatives inhibit the Mild Steel corrosion by adsorption at metal/acid [42, 43]. The inhibition efficiency was calculated from the charge transfer resistance data from equation (3) [44]:

$$\% \ IE_{EIS} = [1 - (R°ct / Rct)] \times 100 \qquad (3)$$

where R_{oct} and R_{ct} are the charge-transfer resistance values without and with inhibitor, respectively.

Fig. 3: Equivalent circuit model used to fit experimental EIS. (3)

TABLE 3

ELECTROCHEMICAL KINETIC PARAMETERS OBTAINED BY EIS TECHNIQUE FOR MILD STEEL IN 2 M HCL WITHOUT AND WITH VARIOUS CONCENTRATIONS OF BENZO[D]OXAZOLE DERIVATIVES (1-2) AT 30 ± 0.1 °C

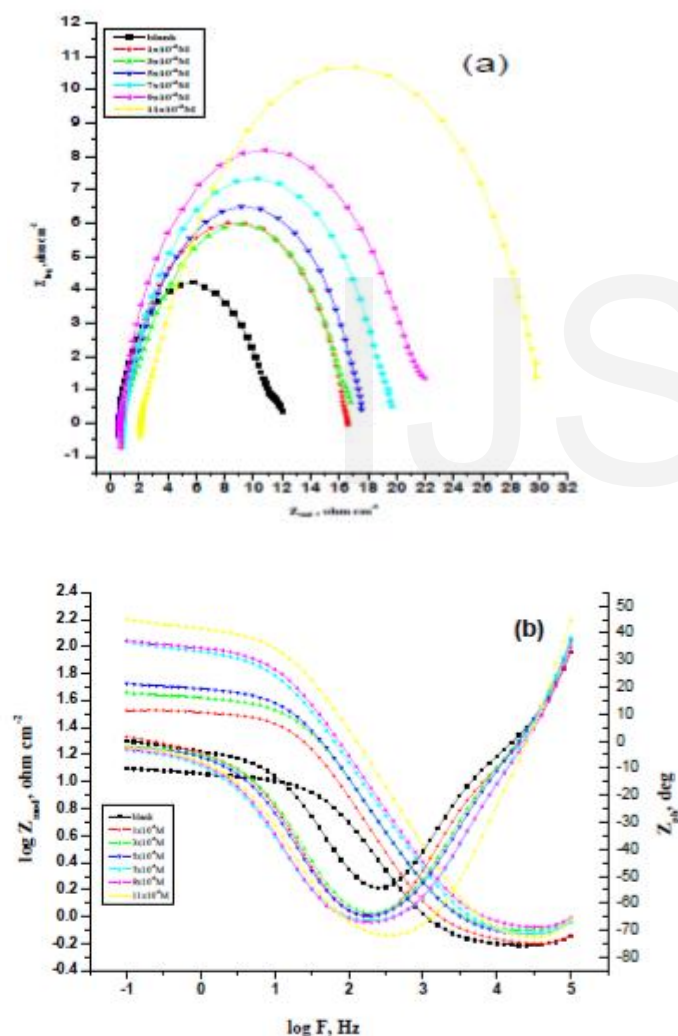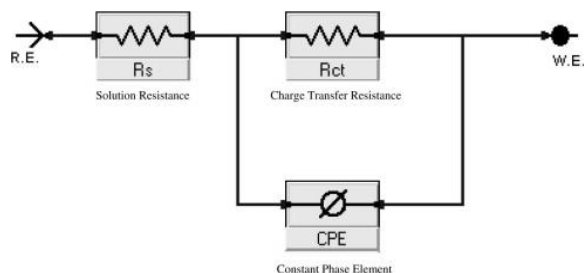| Inhibitors	Conc., M.	R_s, Ω cm^2	Y_0, x 10^{-4} $\mu\Omega^{-1}s^n$	n	R_{ct}, Ω cm^2	C_{dl} X 10^{-4}, μFcm^{-2}	θ	%IE
	Blank	6.2	6.4	8.82	10.77	8.87	------	-----
Compound (1)	1 x 10^{-6}	6.5	4.0	8.77	31.99	2.2	0.6633	66.33
	3 x 10^{-6}	7.9	3.1	8.68	40.50	2.1	0.7340	73.40
	5 x 10^{-6}	7.4	3.3	8.74	49.00	2.0	0.7802	78.02
	7 x 10^{-6}	7.2	2.9	8.62	96.00	1.9	0.8878	88.78
	9 x 10^{-6}	8.3	2.5	8.65	102.00	1.5	0.8944	89.44
	11x 10^{-6}	6.9	1.3	8.87	135.40	1.3	0.9204	92.04
Compound (2)	1 x 10^{-6}	8.2	3.2	8.46	16.00	5.9	0.3268	32.68
	3 x 10^{-6}	8.0	1.2	8.41	17.01	5.0	0.3668	36.68
	5 x 10^{-6}	6.6	1.7	8.22	17.42	4.8	0.3817	38.17
	7 x 10^{-6}	8.3	10.0	8.26	19.01	2.9	0.4334	43.34
	9 x 10^{-6}	7.5	7.3	8.86	21.03	2.8	0.4878	48.78
	11x 10^{-6}	6.1	2.1	7.73	28.99	2.3	0.6284	62.84

Fig. 2: EIS Nyquist plots (a) and Bode plots (b) for Mild Steel surface in 2 M HCl in the absence and presence of different concentrations of compound (1) at 30 ± 0.1 °C.

3.3. Electrochemical Frequency Modulation Technique (EFM)

EFM is a nondestructive corrosion measurement technique that can directly and quickly determine the corrosion current values without prior knowledge of Tafel slopes, and with only a small polarizing signal. These advantages of EFM technique make it an ideal candidate for online corrosion monitoring [45]. The great strength of the EFM is the causality factors which serve as an internal check on the validity of EFM measurement. The causality factors CF-2 and CF-3 are calculated from the frequency spectrum of the current responses.

Figure (4) shows the EFM Intermodulation spectrums of Mild Steel in 2 M HCl solution containing different concentrations of compound (1). Similar curves were obtained for other compound (not shown). The harmonic and intermodulation peaks are clearly visible and are much larger than the background noise. The two large peaks, with amplitude of about

200 µA, are the response to the 40 and 100 mHz (2 and 5 Hz) excitation frequencies. It is important to note that between the peaks there is nearly no current response (<100 nA). The experimental EFM data were treated using two different models: complete diffusion control of the cathodic reaction and the "activation" model. For the latter, a set of three non-linear equations had been solved, assuming that the corrosion potential does not change due to the polarization of the working electrode [46]. The larger peaks were used to calculate the corrosion current density (i_{corr}), the Tafel slopes (βc and βa) and the causality factors (CF-2 and CF-3). These electrochemical parameters were listed in Table (4).

The data presented in Table (4) obviously show that, the addition of any one of tested compounds at a given concentration to the acidic solution decreases the corrosion current density, indicating that these compounds inhibit the corrosion of Mild Steel in 2 M HCl through adsorption. The causality factors obtained under different experimental conditions are approximately equal to the theoretical values (2 and 3) indicating that the measured data are verified and of good quality. The inhibition efficiencies% IE_{EFM} increase by increasing the inhibitor concentrations and was calculated as from equation (4):

$$\%IE_{EFM} = [1-(i_{corr}/i^{\circ}_{corr})]x\ 100 \qquad (4)$$

where i_{ocorr} and i_{corr} are corrosion current densities in the absence and presence of inhibitor, respectively.

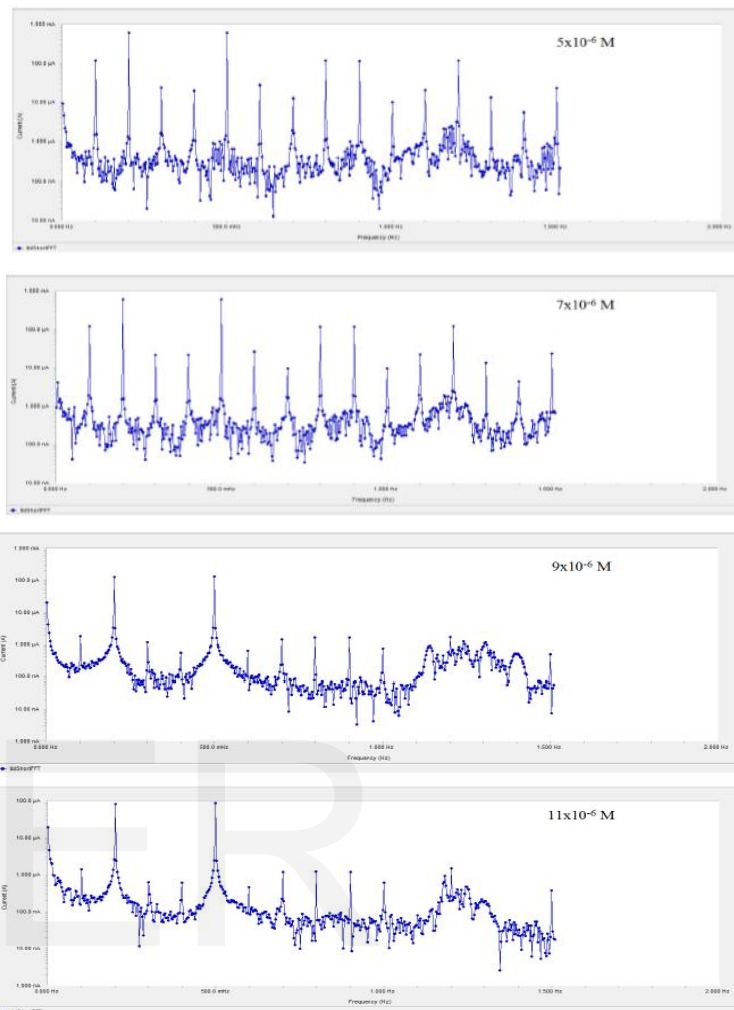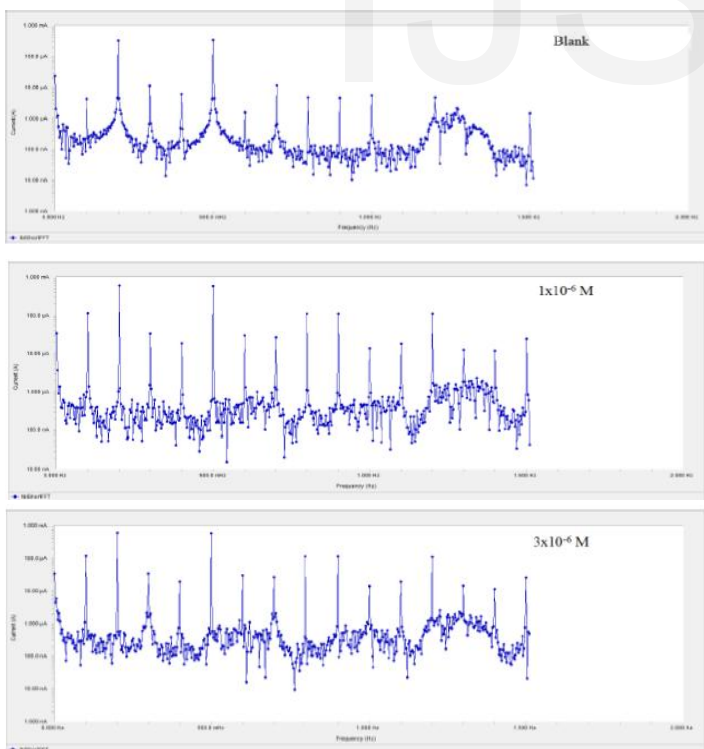The inhibition sufficiency obtained from this method is in the order: compound (1) > compound (2)

Fig. 4. EFM spectra for Mild Steel in 2 M HCl in the abscence and presence of different concentration of compound (1) at 30 ± 0.1 °C.

TABLE 4

ELECTROCHEMICAL KINETIC PARAMETERS OBTAINED BY EFM TECHNIQUE FOR MILD STEEL IN 2 M HCL WITHOUT AND WITH VARIOUS CONCENTRATIONS OF BENZO[D]OXAZOLE DERIVATIVES (1-2) AT 30 ± 0.1 °C.

Inhibitors	Conc., M.	i_{corr}, µA cm^2	$\beta a \times 10^{-3}$, mV dec^{-1}	$\beta c \times 10^{-3}$, mV dec^{-1}	CF-2	CF-3	θ	%IE
	Blank	518.6	911	107	1.8	3.1	-	-
Compound (1)	1 x 10^{-6}	244.4	264	272	2.2	3.0	0.5287	52.87
	3 x 10^{-6}	239.1	261	282	1.7	3.2	0.5389	53.89
	5 x 10^{-6}	232.4	287	271	2.0	2.8	0.5518	55.18
	7 x 10^{-6}	227.9	263	277	2.1	2.6	0.5605	56.05
	9 x 10^{-6}	189.4	981	109	1.9	3.0	0.6347	63.47
	11x 10^{-6}	109.8	888	963	2.0	3.1	0.7882	78.82
Compound (2)	1 x 10^{-6}	253.7	275	321	1.9	3.2	0.5107	51.07
	3 x 10^{-6}	251.8	292	289	1.8	2.9	0.5144	51.44
	5 x 10^{-6}	249.7	287	277	1.9	2.7	0.5185	51.85
	7 x 10^{-6}	246.7	266	268	1.8	3.2	0.5242	52.42
	9 x 10^{-6}	242.0	287	292	2.2	2.9	0.5333	53.33
	11x 10^{-6}	233.1	291	274	2.0	3.4	0.5505	55.05

Figure (5) represents the molecular orbital plots and Mulliken charges of investigated benzo[d]oxazole derivatives. Theoretical calculations were performed for only the neutral forms, in order to give further insight into the experimental results. Values of quantum chemical indices such as energies of lowest unoccupied molecular orbitals (LUMO) and energy of highest occupied molecular orbitals (HOMO) (E_{HOMO} and E_{LUMO}, and energy gap (ΔE) are calculated and given in Table (5). It has been reported that the higher or less negative E_{HOMO} is associated of inhibitor, the greater the trend of offering electrons to unoccupied d orbital of the metal, and the higher the corrosion inhibition efficiency, in addition, the lower E_{LUMO}, the easier the acceptance of electrons from metal surface [47]. From Table (5), it is clear that ΔE obtained by the three methods in case of compound (2) is lower than compound (1), which enhance the assumption that compound (1) molecule will absorb more strongly on Mild Steel surface than compound (2), due to facilitating of electron transfer between molecular orbital HOMO and LUMO which takes place during its adsorption on the Mild Steel surface and thereafter presents the maximum of inhibition efficiency.

Also it can be seen that E_{HOMO} increases from compound (1) to compound (2) facilitates the adsorption and the inhibition by supporting the transport process through the adsorbed layer. Reportedly, excellent corrosion inhibitors are usually those organic compounds who are not only offer electrons to unoccupied orbital of the metal, but also accept free electrons from the metal [48,49]. It can be seen that all calculated quantum chemical parameters validate these experimental results.
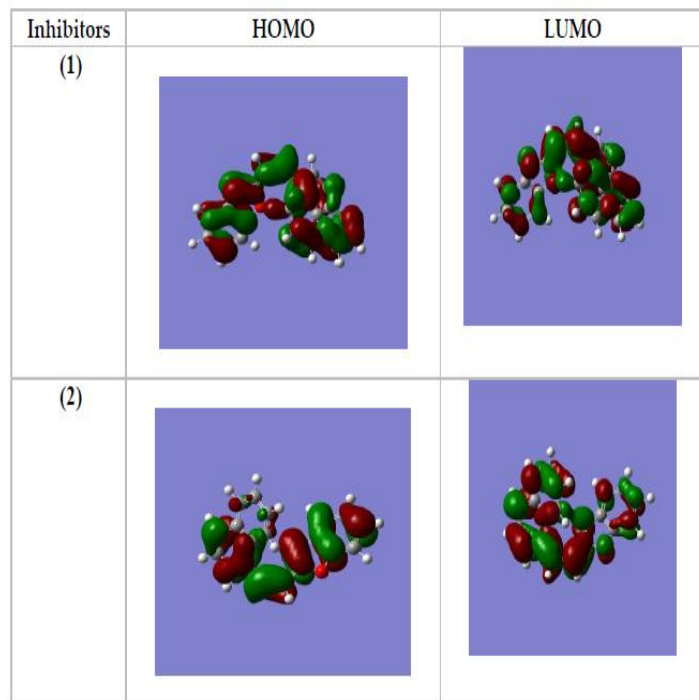
TABLE.4

THE CALCULATED QUANTUM CHEMICAL PROPERTIES FOR INVESTIGATED BENZO[D]OXAZOLE DERIVATIVES.

	Compound (1)	Compound (2)
$-E_{HOMO}$ (a.u)	0.2952	0.3014
$-E_{LUMO}$ (a.u)	0.2253	0.2167
ΔE (a.u)	0.070	0.085
η (a.u)	0.035	0.042
σ (a.u)$^{-1}$	28.612	23.613
-Pi (a.u)	0.260	0.259
χ (a.u)	0.260	0.259

3.5. Molecular Docking

Molecular docking is a key tool in computer drug design [50-53]. The focus of molecular docking is to simulate the molecular recognition process. Molecular docking aims to achieve an optimized conformation for both the protein and drug with relative orientation between them such that the free energy of the overall system is minimized. In this context, we used molecular docking between compounds (1-2) and receptor of breast cancer mutant 3hb5-oxidoreductase. The results showed a possible arrangement between compounds (1-2) and 3hb5 receptor. The docking study showed a favorable interaction between compounds (1-2) and the receptor (3hb5) as shown in Figure. (6) and the calculated energy is listed in Table (6). According to the results obtained in this study, HB plot curve indicates that the compounds (1-2) binds to the proteins with hydrogen bond interactions and decomposed interaction energies in kcal/mol were exist between compounds (1-2) with 3hb5 receptor as shown in Figure (7). 2D plot curves of docking with compounds (1-2) are shown in Figure (8).
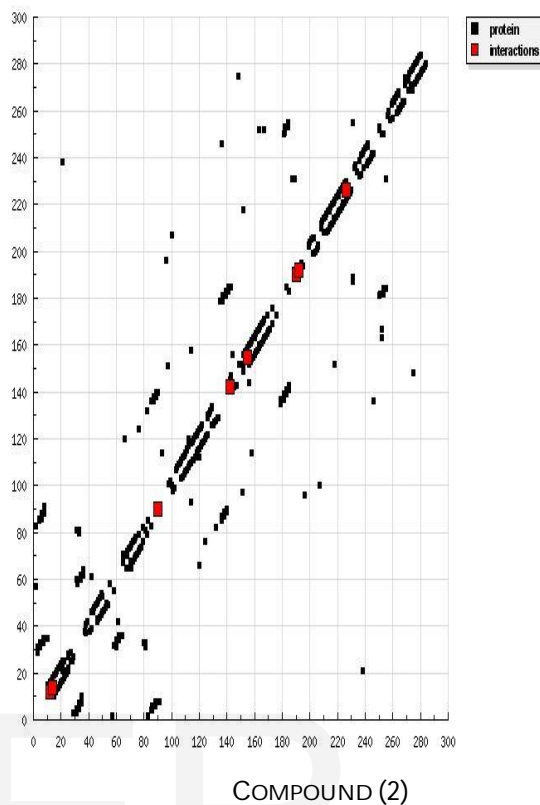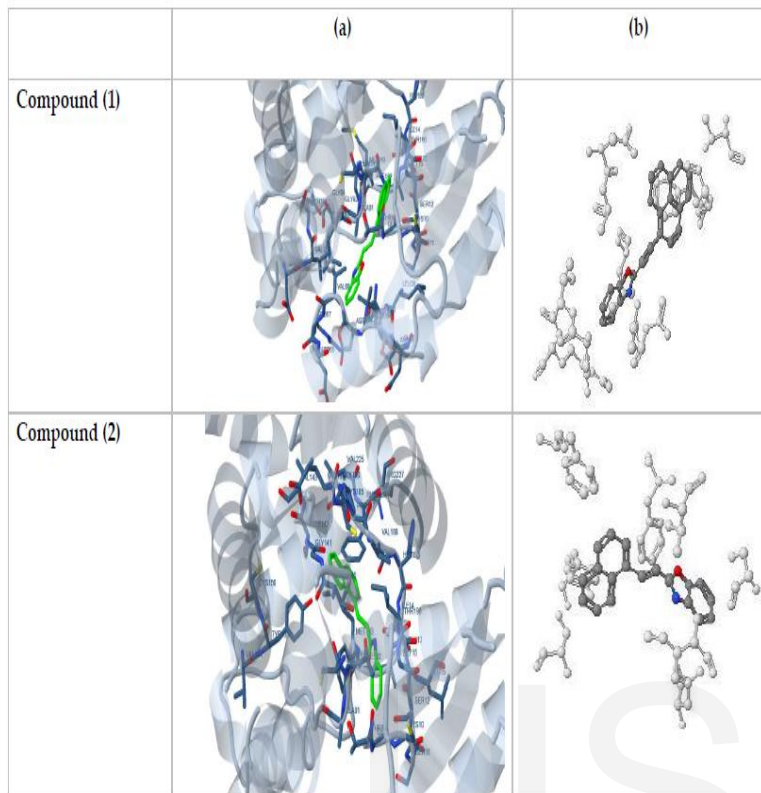

Fig. 5. Molecular orbital plots of investigated benzo[d]oxazole derivatives.

	(a)	(b)
Compound (1)		
Compound (2)		

COMPOUND (2)

Interactions	
12:	SER
14:	ILE
90:	ASN
142:	SER
155:	TYR
190:	THR
192:	PHE
226:	PHE

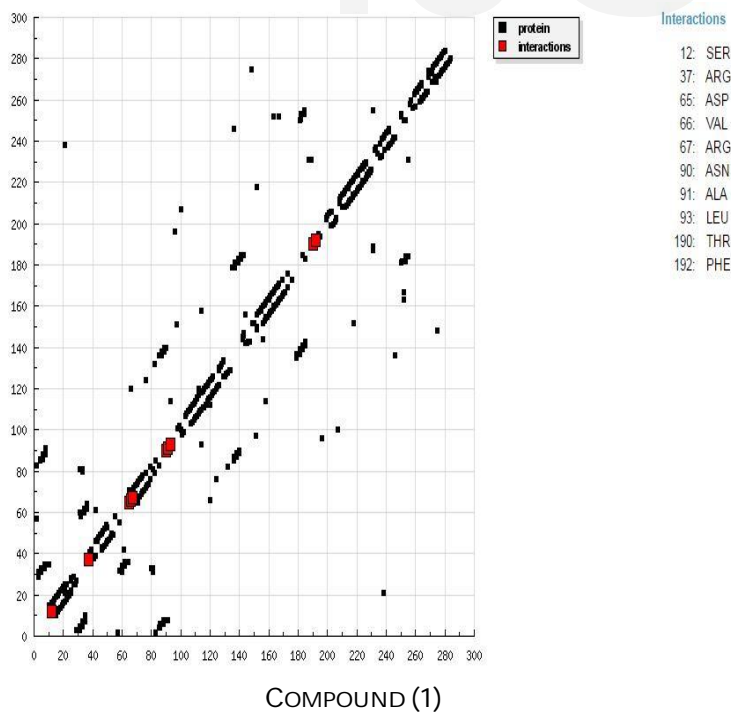Fig. 7. HB plot of interaction between compounds (1-2) and receptor of breast cancer mutant 3hb5-oxidoreductase.

COMPOUND (1)

Interactions	
12:	SER
37:	ARG
65:	ASP
66:	VAL
67:	ARG
90:	ASN
91:	ALA
93:	LEU
190:	THR
192:	PHE

Key

COMPOUND (1)

Key

COMPOUND (2)

Fig. 8. 2D plot of interaction between compounds (1-2) and receptor of breast cancer mutant 3hb5-oxidoreductase.

TABLE 6

ENERGY VALUES OBTAINED IN DOCKING CALCULATIONS OF BEN-ZO[D]OXAZOLE DERIVATIVES WITH RECEPTOR OF BREAST CANCER MUTANT 3HB5-OXIDOREDUCTASE

Compound	Est. Free Energy of Binding (kcal/mol)	Est. inhibition constant (K_i) (μM)	vdW+ bond+ desolv energy (kcal/mol)	Electrostatic Energy (kcal/mol)	Total intercooled Energy (kcal/mol)	Interact surface
(1)	-8.25	896.61	-8.79	-0.04	-8.83	811.377
(2)	-7.91	1.59	-8.48	-0.03	-8.50	780.355

3.6. Chemical Structure of the Inhibitors and Corrosion Inhibition

Inhibition of the corrosion of Mild Steel in 2 M HCl solution by some benzo[d]oxazole derivatives is determined by potentiodynamic anodic polarization measurements, Electrochemical Impedance Spectroscopy (EIS) and electrochemical frequency modulation method (EFM) Studies, it was found that the inhibition efficiency depends on concentration, nature of metal, the mode of adsorption of the inhibitors and surface conditions.

The observed corrosion data in presence of these inhibitors, namely:

The decrease of corrosion rate and corrosion current with increase in concentration of the inhibitor.

The shift in Tafel lines to higher potential regions.

The inhibition efficiency depends on the number of adsorption active centers in the molecule and their charge density.

It was concluded that the mode of adsorption depends on the affinity of the metal towards the π-electron clouds of the ring system. Metals such as Fe, which have a greater affinity towards aromatic moieties, were found to adsorb benzene rings in a flat orientation. The order of decreasing the percentage inhibition efficiency of the investigated benzo[d]oxazole derivatives in the corrosive solution was as follow: compound (1) > compound (2). Compound (1) exhibits excellent inhibition power due to its larger molecular size that may facilitate better surface coverage. Compound (2) comes after compound (1) in inhibition efficiency. This is due to it has lesser molecular size, which lower the electron density on the molecule and hence, lower inhibition efficiency.
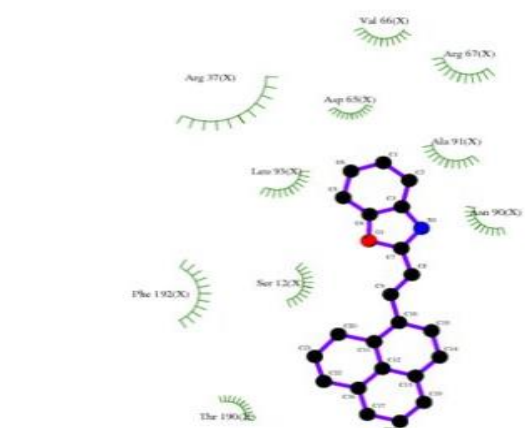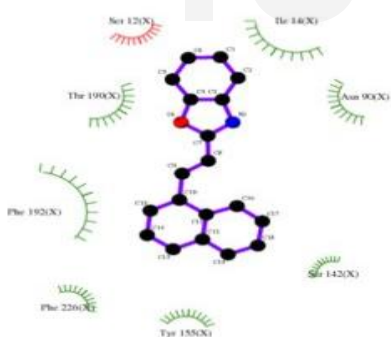
4 CONCLUSION

1- All the investigated benzo[d]oxazole derivatives are good corrosion inhibitors for Mild Steel in 2 M HCl solution. The effectiveness of these inhibitors depends on their structures. The variation in inhibitive efficiency depends on the type and the nature of the substituent present in the inhibitor molecule.

3- Double layer capacitances decrease with respect to blank solution when the inhibitor added. This fact may be explained by adsorption of the inhibitor molecule on the Mild Steel surface.

4- EFM can be used as a rapid and nondestructive technique for corrosion measurements without prior knowledge of Tafel slopes

5- The order of % IE of these investigated compounds is in the following order: compound (1) > compound (2).

6- Quantum chemistry calculation results showed that the heteroatoms of N and O are the active sites of the benzo[d]oxazole compounds. It can adsorb on Fe surface firmly by donating electrons to Fe atoms and accepting electrons from 3d orbital of Fe atoms.

7- Molecular docking was used to predict the binding between benzo[d]oxazole derivatives (1-2) and the receptor of breast cancer mutant 3hb5-oxidoreductase.

REFERENCES

[1]. Wahdan M.H., Hermas A.A., Morad M.S., Mater. Chem. Phys. 76 (2002) 111-118.

[2]. Bentiss F., Lebrini M., Vezin H., Lagrenee M., Mater. Chem. Phys. 87 (2004) 18-23.

[3]. Liu X., Okafor P.C., Zheng Y.G., Corros. Sci. 51 (2009) 744-751.

[4]. Al Maofari A., Ezznaydy G., Idouli Y., Guedira F., Zaydoun S., Labjar N. and El Hajjaji S., *J. Mater. Environ. Sci. 5 (2014) 2081- 2085.*

[5]. Barouni K., Kassale A., Albourine A., Jbara O., Hammouti B., Bazzi L., *J. Mater. Environ. Sci. 5* (2014) *456-463.*

[6]. Fouda A.S., Shalabi K., Elmogazy H., J. Mater. Environ. Sci. 5 (2014) 1691-1702.

[7]. Ostovari A., Hoseinieh S.M., Peikari M., Shadizadeh S.R., Hashemi S.J., Corros. Sci. 51 (2009) 1935-1949.

[8]. Bahrami M.J., Hosseinia S.M.A., Pilvar P., Corros. Sci. 52 (2010) 2793-2803.

[9]. Solomon M.M., Umoren S.A., Udosoro I.I., Udoh A.P., Corros. Sci. 52 (2010) 1317-1325.

[10]. Wang H.L., Liu R.B., Xin J., Corros. Sci. 46(2004) 2455-2466.

[11]. Solmaz R., Kardas G., Yazici B., Erbil M., Prot. Met. 41 (2005) 581-585.

[12]. Emregul K.C., Kurtaran R., Atakol O., Corros. Sci. 45 (2003) 2803-2817.

[13]. Chebabe D., Chikh Z.A., Hajjaji N., Srhiri A., Zucchi F., Corros. Sci. 45 (2003) 309-320.

[14]. Liu F.G., Du M., Zhang J., Qiu M., Corros. Sci. 51 (2009) 102-109.

[15]. Musa A.Y., Kadhum A.A.H., Mohamad A.B., Takriff M.S., Corros. Sci. 52 (2010) 3331-3340.

[16]. Khaled K.F., Amin M.A., Corros. Sci. 51 (2009) 1964-1975.

[17]. Quraishi M.A., Rafiquee M.Z.A., Khan S., Saxena N., J. Appl. Electrochem. 37 (2007) 1153-1162.

[18]. Zhang X.Y., Wang F.P., He Y.F., Du Y., Corros. Sci. 43 (2001)1417-1431.

[19]. Knag M., Bilkova K., Gulbrandsen E., Carlsen P., Sjoblöm J., Corros. Sci. 48 (2006) 2592-2613.

[20]. Wang L., Yin G.J., Yin J.G., Corros. Sci. 43 (2001) 1197-1202.

[21]. Okafor P.C., Liu X., Zheng Y.G., Corros. Sci. 51 (2009) 761-768.

[22]. Zhang J., Liu J.X., Yu W.Z., Yan Y.G., You L., Liu L.F., Corros. Sci. 52 (2010) 2059-2065.

[23]. Eldesoky A.M., El-Bindary M.A., El-Sonbati A.Z., Morgan Sh.M., J. Mater. Environ. Sci. 6 (2015) 2260-2276.

[24]. Kassou O., Galai M., Ballakhmima R. A., Dkhireche N., Rochdi A., Ebn Touhami M., Touir R., Zarrouk A., *J. Mater. Environ. Sci. 6 (2015) 1147-1155.*

[25]. Eldesoky A.M., Diab M.A., El-Bindary A.A., El-Sonbati A.Z., Seyam H.A., J. Mater. Environ. Sci. 6 (2015) 2148-2165.

[26]. Halgren T. A., J. Computat. Chem. 17 (1998) 490-519.

[27]. Morris. G.M., Goodsell. D.S., J. Comput. Chem. 19 (1998) 1639-1662.

[28]. Aiello.S., Wells.G., Stone.E.L., Kadri.H., Bazzi. R., J. Med. Chem., 51 (2008) 5135–5139.

[29]. Lorenz W.J., Mansfeld F., Corros. Sci. 21 (1981) 647-672.

[30]. Putilova I.N., Balezin S.A., Barannik V.P., "Metallic Corrosion Inhibitors Pergamon" Press NewYork, 1960.

[31]. Al-Neami K.K., Mohamed A.K., Kenawy I.M., Fouda A.S., Monatsh. Chem. 126 (1995) 369- 376.

[32]. Noor E.A., Int. J. Electrochem. Sci. 2(2007)996-1017.

[33]. Marsh J., Advanced Organic Chemistry 3rd ed Wiley Eastern New Delhi (1988).

[34]. Martinez S., Stern I., Appl.Surf.Sci. 199 (2002) 83-89.

[35]. Al-Khaldi M. A., Al-qahtani K. Y. J. Mater. Environ. Sci. 4 (5) (2013) 593-600.

[36]. Schltze J.W., Wippermann K., Electrochim. Acta 32 (1987) 823-831.

[37]. Silverman D.C., Carrico J.E., Corrosion 44 (1988) 280- 287.

[38]. Macdonald D.D., Mckubre M.C.H., "Impedance measurements in electrochemical systems" Modern Aspects of Electrochemistry, Bockris J. O'M., Conway B.E., White R.E., Eds., Plenum Press, New York 14 1982 pp. 61–150.

[39]. Mansfeld F., Corrosion 36 (1981) 301-307.

[40]. Gabrielli C., "Identification of Electrochemical processes by Frequency Response Analysis" Solarton Instrumentation Group, 1980.

[41]. El Achouri M., Kertit S., Gouttaya H.M., Nciri B., Bensouda Y., Perez L., Infante M.R., Elkacemi K., Prog. Org. Coat. 43 (2001) 267-273.

[42]. Anejjar A., Zarrouk A., Salghi R., Zarrok H., Ben Hmamou D., Hammouti B., Elmahi B., Al-Deyab S.S., J. Mater. Environ. Sci. 4 (2013) 583-592.

[43]. Mertens S.F., Xhoffer C., Decooman B.C., Temmerman E., Corrosion 53 (1997) 381-388.

[44]. Trabanelli G., Montecelli C., Grassi V., Frignani A., J. Cem. Concr. Res. 35 (2005) 1804-1813.

[45]. Trowsdate A.J., Noble B., Haris S.J., Gibbins I.S.R., Thomson G.E., Wood G.C., Corros. Sci. 38 (1996) 177-191.

[46]. Reis F.m., de Melo H.G., Costa I., J. Electrochem. Acta 51 (2006) 1780-1788.

[47]. Lagrenée M., Mernari B., Bouanis M., Traisnel M., Bentiss F., Corros. Sci. 44 (2002) 573-588.

[48]. McCafferty E., Hackerman N., J. Electrochem. Soc.119 (1972) 999-1009.

[49]. Ma H., Chen S., Niu L., Zhao S., Li S., Li D., J. Appl. Electrochem. 32 (2002) 65-72.

[50]. El-Sonbati A.Z., Mohamed G.G., El-Bindary A.A., Hassan W.M.I., Diab M.A., ElkholyA.K., J. Mol. Liq. 212 (2015) 487–502.

[51]. El-Bindary A.A., Mohamed G.G., El-Sonbati A.Z., Diab M.A., Hassan W.M.I., Morgan Sh.M., Elkholy A.K., J. Mol. Liq. 218 (2016) 138–149.

[52]. El-Sonbati A.Z., El-Bindary A.A., Mohamed G.G., Morgan Sh.M., Hassan W.M.I., Elkholy A.K., J. Mol. Liq. 218 (2016) 16–34.

[53]. Diab M.A., El-Sonbati A.Z., El-Bindary A.A., Morgan Sh.M., Abd El-Kader M.K., J. Mol. Liq. 218 (2016) 571–585.